SURFACE MODIFICATION OF POLYMER SUBSTRATES BY NANOPARTICLES VIA SOLUTION-BASED METHOD

A Thesis

Presented to the Faculty of the Graduate School

of Cornell University

In Partial Fulfillment of the Requirements for the Degree of

Master of Science

by

Yan Kang

August 2012

ABSTRACT

Surface modification is a good way to introduce desired physical, chemical or biological properties to materials without changing the characteristics of the bulk. Modifying polymer surfaces has drawn much attention because this process gives the potential to further increase the versatility of polymer materials.

My work focuses on using colloidal nanoparticles to functionalize polyamide water treatment membranes and polycarbonate plastic sheets with nanoparticles with different purposes. Specifically, modifying polyamide membranes with colloidal copper nanoparticles or positively charged silica are described in the first part of this thesis. Coating polycarbonate sheets with positively charged silica nanoparticles is discussed in the second part. Fabrication and characterization of these nanoparticle functionalized substrates will be emphasized.

BIOGRAPHICAL SKETCH

Yan Kang was born on January 18th, 1988 in Langfang, a small city of Hebei Province, China. After several moves in Hebei Province with the family, he moved to Beijing in 2003. In 2006, he joined Tsinghua University for his undergraduate study in Materials Science and Engineering. After he graduated with a Bachelor of Engineering degree in 2010, he continued his study at Cornell University as a master student. He is extremely grateful for all his previous experiences and believes in a better future.

To my beloved family and dear friends

ACKNOWLEDGMENTS

I will always appreciate the guidance, encouragement and support of my advisor, Professor Emmanuel Giannelis, over the past two years. I am grateful as well for having had the opportunity to work with many other past and present members in the Giannelis Groups. Their kind assistance is invaluable to me.

I would also like to express my gratitude to Professor Richard Hennig for serving on my committee and giving me useful advices. I would like to further extend my appreciation to Professor Michael Thompson, Professor Jack Blakely and other professors who performed enlightening instructions in my academic courses. My thanks shall go to Professor Menachem Elimelech and his group at Yale University for their great help in our collaborative projects.

I have greatly benefited from the communities and all the staff at Cornell University. I would like to say thanks to all of them in the Department of Materials Science and Engineering (Michelle Conrad, Carol Armstrong, Karen Jordan etc.), KAUST-Cornell Center for Energy and Sustainability (David Jung, Celia Szczepura, Angela Yontz, Brenda Fisher), Cornell Center of Materials Research (Jon Shu, Mick Thomas, John Sinnott, John Hunt etc.). Furthermore, I own many thanks to my friends who brought me many wonderful moments and made my stay in Ithaca memorable.

Last but not the least I want to show my deepest gratitude to my parents. Without their support and love, nothing could have been done. I dedicate my thesis to them.

TABLE OF CONTENTS

LIST OF FIGURES

LIST OF TABLES

CHAPER I

MODIFYING SURFACE OF POLYAMIDE WATERTREATMENT MEMBRANES

1.1 Introduction

In this chapter, coating nanoparticles on the surface of thin-film composite polyamide membranes is mainly discussed. In water treatment industry for desalination or wastewater reuse, membrane-based technologies play a critical part. Polyamide thin-film composite membranes are currently at the core part in this industry [1, 2]. The membranes are semipermeable to retain contaminants in one side while pure water goes to the other side. One big challenge for the membranes is fouling resulted from dissolved molecules, particulates and microorganisms in the feed streams [3]. Efforts have been made to reduce and/or delay the fouling, for example, tailoring chemistry or morphology of the polyamide membranes by adding monomers or changing conditions during interfacial polymerization in membrane synthesis [4, 5]. This pathway has limited range of improvements in industry-scale production and increases uncertainties of products after polymerization reaction. As a result, to functionalize the post-fabricated membranes with novel materials is more desirable.

Various coatings, primarily nanoparticles such as biocidal Ag [6-8], photocatalytic TiO_2 [9, 10] and iron [11], have been tried for water treatment membranes. This strategy to promote membrane antifouling through functionalizing thin-film

membranes with active nanomaterials is promising. The present work focuses on grafting copper nanoparticles, which is a fairly cheap material, through capping the particles with polymers. Moreover, coating super-hydrophilic silica nanoparticles is another important approach to render desirable functionalities to polyamide membranes, with the purpose of rendering the surface more hydrophilic, smooth and less charged. Figure 1.1 shows the schematics of these two approaches. More details will be discussed in this chapter.

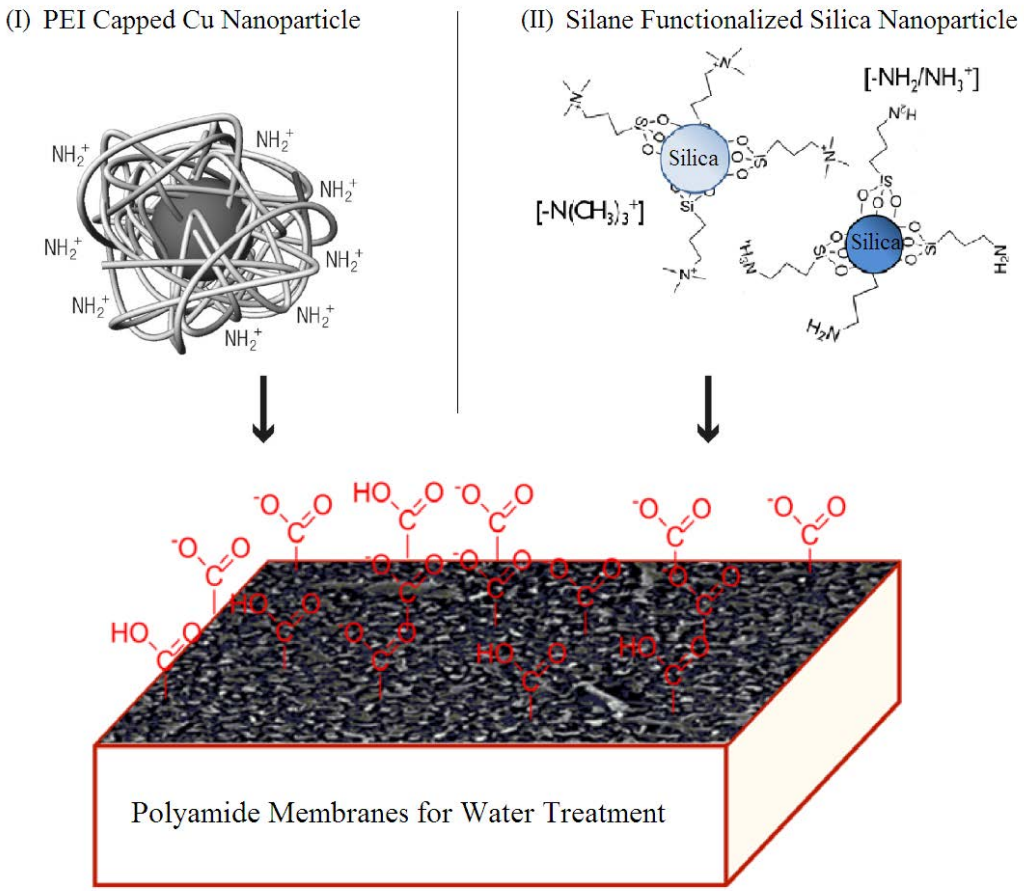

Figure 1.1: Schematic of the two approaches to coat the polyamide membranes with copper or silica nanoparticles.

The polyamide thin-film membranes were prepared on polysulfone (PSf) ultrafiltration membrane supports by interfacial polymerization between m-phenylenediamine and trimesoyl chloride [12]. From this way the membranes were equipped with native carboxylic groups at the surfaces, about 20 –COOH per planar square nanometers from top view (polyamide membranes are very rough, in each 1 nm^2 of planar area there are many nm^2 of actual surface). These carboxylic groups are negatively charged when in aqueous solution and can be exploited as binding sites for functionalized nanoparticles. The polyamide membranes were hand-casted by the Elimelech Group at Yale University.

1.2 Surface Modification of Polyamide Membranes via Grafting Copper Nanoparticles

1.2.1 Preparation of Colloidal Copper Nanoparticles

Positively charged copper particles were synthesized in a three-step process. First, 5 mM $CuSO_4$ solution was mixed with an equal volume of 0.075g poly(ethyleneimine) (PEI, M_w = 60,000 g•mol^{-1}), yielding a blue solution. Then, 0.16 g $NaBH_4$ was quickly added and the solution was vigorously stirred until there were no hydrogen bubbles generated. Finally, the solution was dialyzed using SnakeSkin tubing (10,000 MWCO, Pierce) for 3 days to remove excess reactants, and a dark green solution of PEI-capped copper nanoparticles (PEI-CuNPs) was prepared for further experiments. X-ray Diffraction (XRD, Scintag Theta-Theta X-ray Diffractometer PAD-X) was used for

compound identification. Particle size was characterized via transmission electron microscopy (TEM, FEI Tecnai F20, Hillsboro, OR). The electrophoretic mobility was determined using a dynamic light scattering and zeta potential analyzer (Malvern Zetasizer Nano-ZS, Worcestershire, UK). The tests were performed in deionized water from millipore purification system with a specific conductance of 0.05 $\mu S \cdot cm^{-1}$ and pH 5.5. All chemicals were purchased from Sigma-Aldrich (St. Louis, MO).

The TEM image of the particles, as shown in Figure 1.2, shows the average diameter of the particles is around 10 nm with good distribution. In dynamic light scattering measurement, the average diameter of the particles is also around 10 nm. The PEI-CuNPs solution was diluted to 15 times of the volume and sonicated for 15 min for the dynamic light scattering measurement. The zeta potential is about 30.7 mV. The XRD pattern is shown in Figure 1.3. Red lines indicate where the peaks for cuprite (Cu_2O) should appear while blue indicate the positions for metallic copper (Cu). Most likely the synthesis process described above yielded core/shell nanoparticles with metallic copper covered by oxidized copper (cuprite) due to the good affinity of copper surface to oxygen.

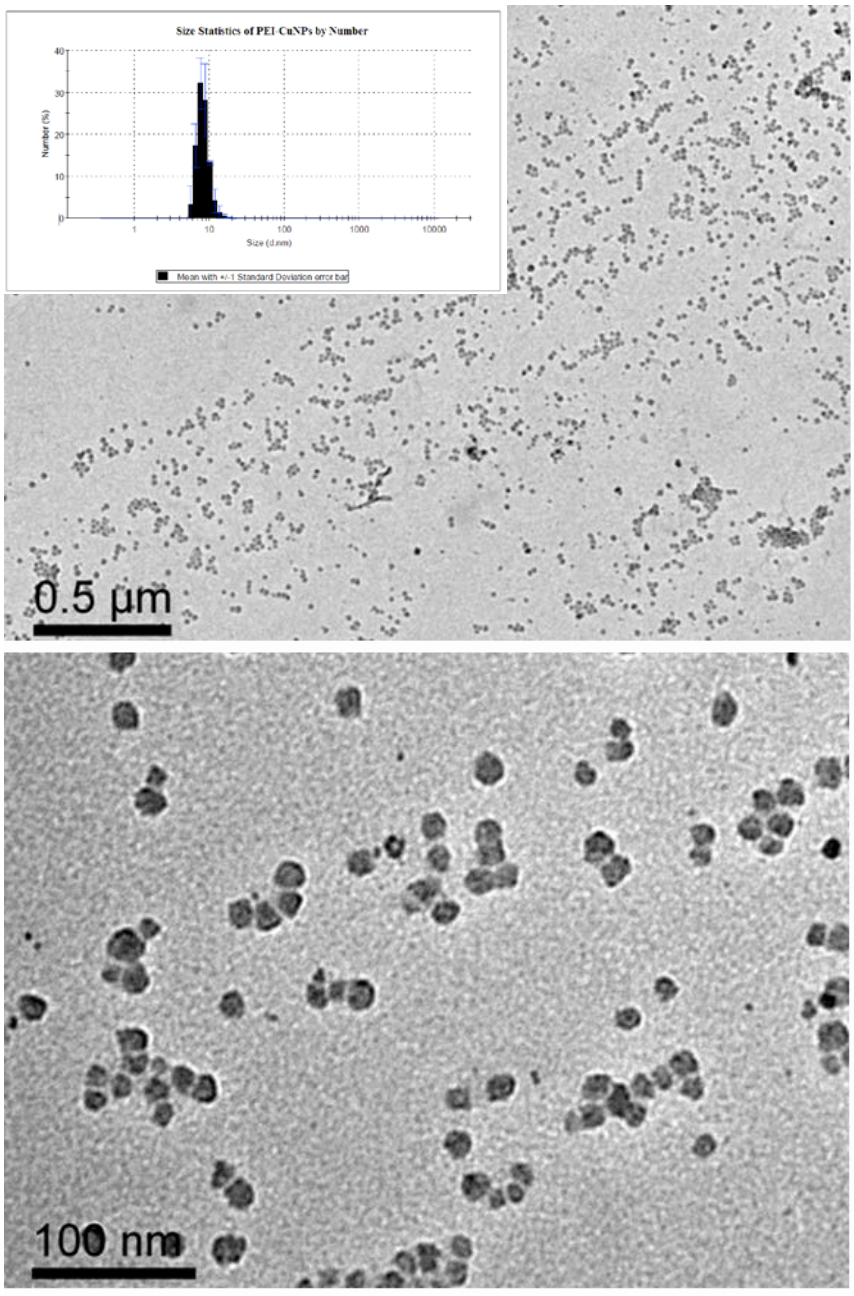

Figure 1.2: TEM image and dynamic light scattering size statistics of PEI-capped Copper Nanoparticles.

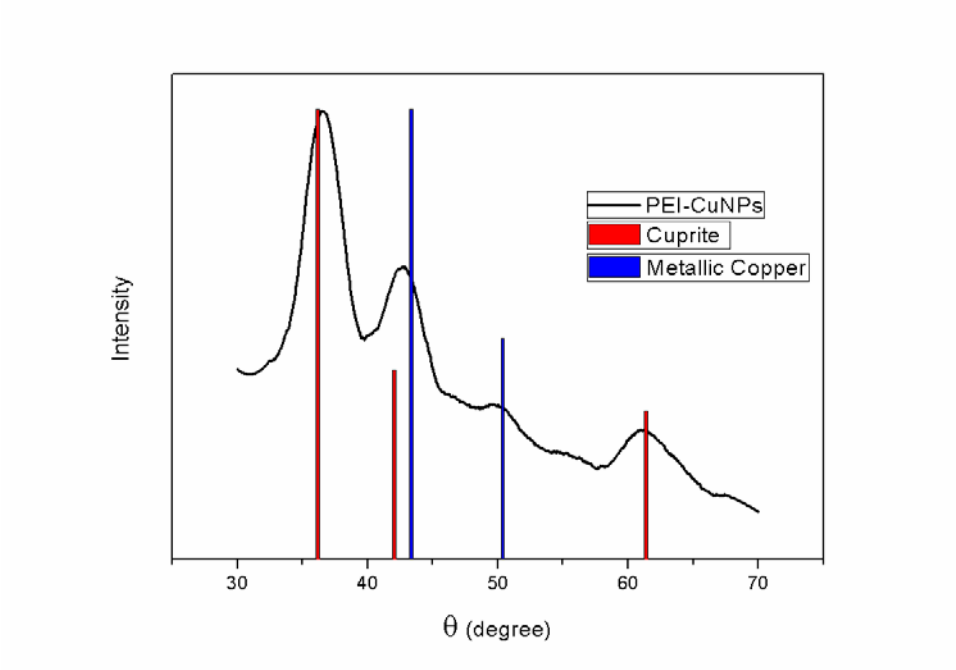

Figure 1.3: XRD pattern of PEI-capped Copper Nanoparticles. Red lines indicate where the peaks for cuprite (Cu_2O) should appear and blue lines indicate the positions for metallic copper (Cu).

1.2.2 Coating Process

The polyamide thin-film membranes possess free carboxylic groups, so nanoparticles covered with amine-terminals can ionically bonded to the surfaces by a simple dip-coating process, which was to directly immerse the membranes in solutions of PEI-capped copper nanoparticles for 16 hours at room temperature.

1.2.3 Results and Discussion

The surface of polyamide membranes were examined via various tools including X-ray photoelectron spectroscopy (XPS, Surface Science Instrument SSX-100 UHV, monochromated for Al Kα X-rays with 1486.6 eV), scanning electron microscopy (SEM, LEO 1550 FESEM).

The spectra of XPS survey scans for the membranes are presented in Figure 1.4. Compared with uncoated polyamide membranes, a prominent peak for Cu (Binding energy ~ 933 eV) is observed, confirming the binding of Cu at the surface. The atomic fraction for Cu is about 1%. SEM images are presented in Figure 1.5.

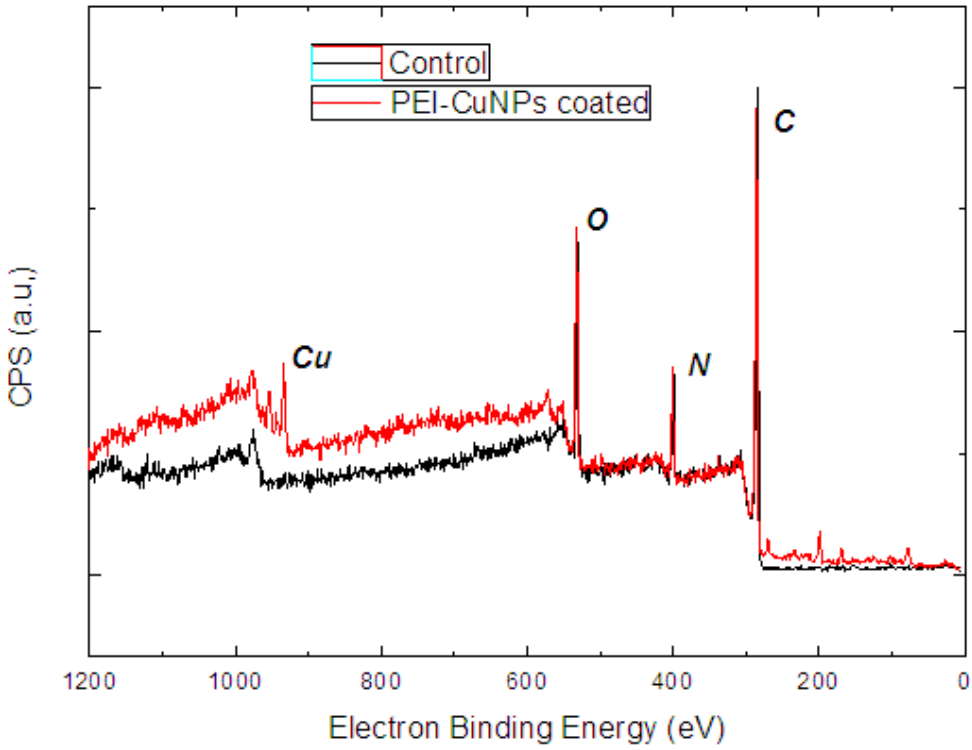

Figure 1.4: XPS spectra of neat polyamide membranes and PEI-CuNPs grafted polyamide membranes.

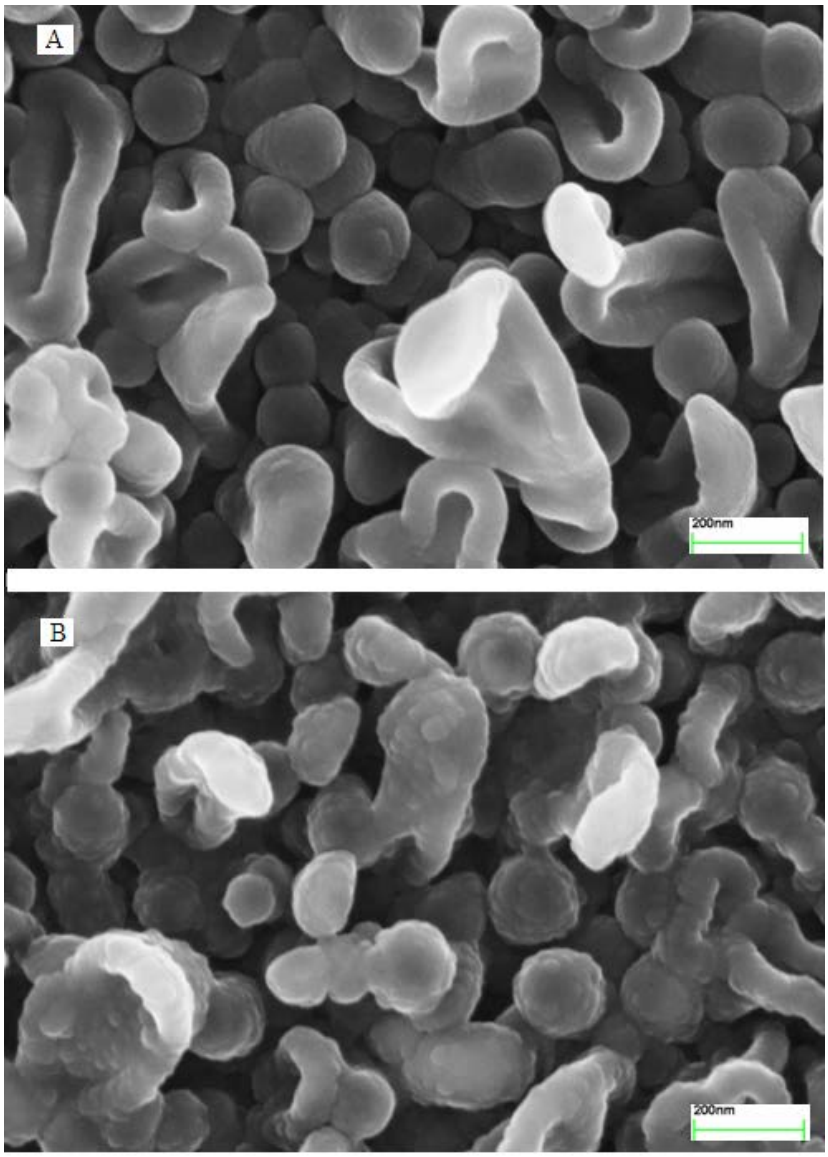

Figure 1.5: SEM images for (A) control membranes and (B) PEI-CuNPs grafted membranes.

1.2.4 Fouling Behavior

The way to test the antimicrobial behavior (inactivation effect for fouling) of the coated membranes was to have the membranes contacted with *Escherichia coli K12* (a kind of kanamycin resistant bacterium) and then to measure the cell density after aging. Specifically, the *Escherichia coli K12* grew overnight in 1% mannose minimal media solution. The cells were rinsed with the concentrated mannose growth media and resuspended in isotonic solution. The active side of the membrane was placed in contact with the cell suspension for one hour at 37 ºC. After incubation, the membranes were rinsed again and sonicated. Different dilution rates (10^{-1}, 10^{-2}, and 10^{-3}) of the resulting cells with Luria Broth agar and kanamycin were used after 1 hour of growth. The inactivation rates of the membranes were then measured and determined by comparing the cell density of the modified membranes and the control membranes. Figure 1.6 gives the numeric result of living colonies after 1 hour growth. The blue rectangle stands for the control group of neat membranes while the red rectangle stands for PEI-CuNPs coated membranes. Clearly, the living cells on control membranes were significantly more than those on the modified membranes. Good antimicrobial activity is proved for the PEI-CuNPs coated membranes. The fouling experiments were performed by the Elimelech Group at Yale University.

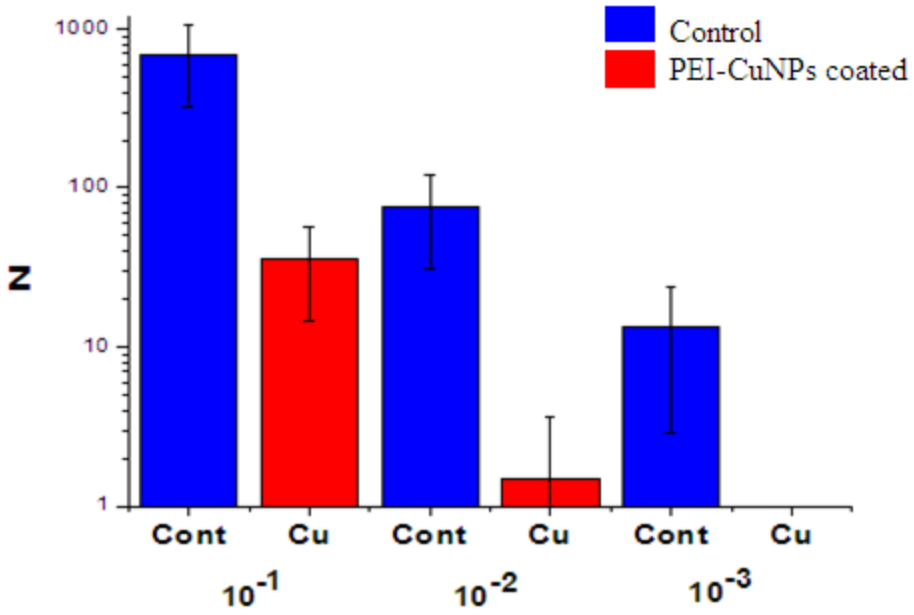

Figure 1.6: Number of living bacterial cells on PEI-CuNPs coated membranes and unmodified membranes after 1 hour growth.

1.3 Surface Modification of Polyamide Membranes with Silica-based Nanoparticles

1.3.1 Preparation of Positively Charged Silica Nanoparticles

Two kinds of positively charged silica nanoparticles functionalized with amine ends were synthesized. A two-step process was used to synthesize the functionalized silica nanoparticles taking advantage of the silation reaction between silanes and hydroxyls on the silica surface. Specifically, 3 g of commercial silica colloid (HS-30, 30 wt% suspension in water, Ludox) was firstly diluted with 27 g of deionized water and sonicated for 30 min. Then two kinds of silanes, 3.2 g of N-Trimethoxysilylpropyl-N,N,N-Trimethylammonium chloride (50 wt% in methonal, Gelest) with quaternary ammonium ends or 1.2 g of (3-Aminopropyl)trimethoxysilane (97%, Sigma-Aldrich) with primary amine ends, were mixed with the sonicated silica suspension for obtaining two different kinds of functionalized silica nanoparticles. The mixture containing silica nanoparticles and silanes were continuously stirred and heated at 70ºC for 24 hours. When making silica nanoparticles with primary amine ends, the pH of the blend solution was changed to ~5 by 0.1 M HCl before heating. After heating, the solutions became transparent and then were dialyzed for 48 hours using SnakeSkin tubing (7,000 MWCO, Pierce) for removing excess reactants. The pH of the final solutions were ~8 for silica nanoparticles functionalized with quaternary ammonium ("Silica-Quats"), and ~6 for silica nanoparticles functionalized with primary amine ("Silica-NH_2"), respectively. The products were evaluated with transmission electron

microscopy (TEM, FEI Tecnai F20, Hillsboro, OR), Thermogravimetric Analyzer with Differential Thermal Analysis (TG/DTA, EXSTAR TG/DTA 6200 series), zeta potential measurement (Malvern Zetasizer Nano-ZS, Worcestershire, UK).

As indicated in TEM images (Figure 1.7), both of the two products - silica nanoparticles functionalized with quaternary ammonium (Silica-Quats) and silica nanoparticles functionalized with primary amine (Silica-NH_2) - have a particle size in the range of 15 - 22 nm. This result corresponds well with the dynamic light scattering experiments, which give a mean size of ~18 nm. The zeta potential of the as-prepared Silica-Quats is around 30.5 mV and 29.3 mV for Silica-NH_2. The organic content data (thermogravimetric study) will be shown in the next chapter (Figure 2.1, Chapter 2).

1.3.2 Coating Process

As described in the introduction of this chapter and in 1.2.2, the polyamide membranes have a considerable number of free carboxylic groups on the surface. The simple dip-coating process which was to directly immerse the membranes in nanoparticle solutions was followed for Silica-Quats. For coating with Silica-NH_2 solution, EDC and NHS were used. The concentration of EDC and NHS were 2 mM and 5 mM, respectively. The neat membranes were immersed in such EDC-NHS solution for 15 minutes and then the active surfaces were rinsed well by deionized water. During this step, the native carboxylate groups at the polyamide surface were converted into intermediate amine-reactive esters for cross-linking [13, 14]. After rinsing excess reactants, the membranes were immersed in Silica-NH_2 solution for 16

hours. A few drops of 0.05M NaOH were used to change the Silica-NH_2 solution to desired working pH range (~7.5) instead of using buffers. The functionalized silica solution could survive and retain its properties in the pH range for EDC-NHS to work.

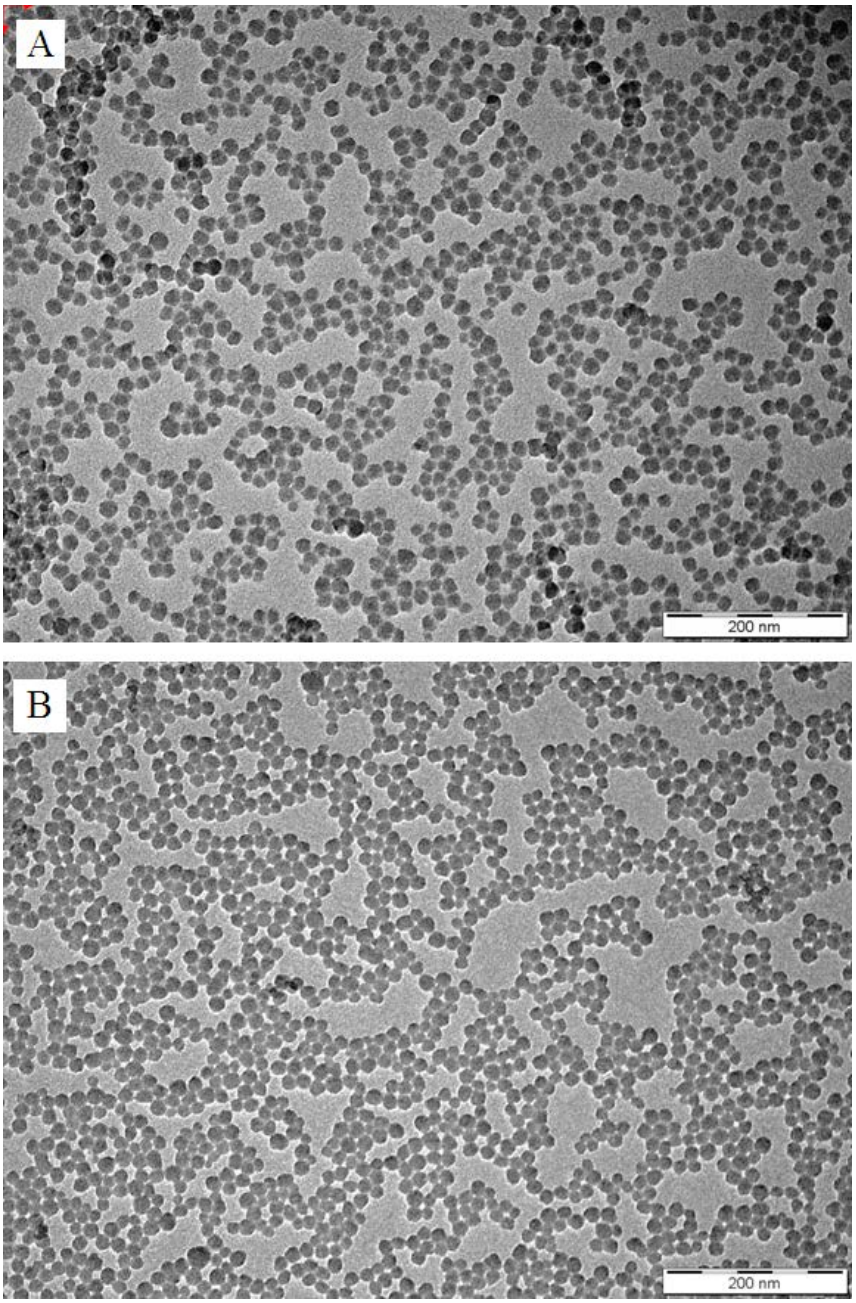

Figure 1.7: TEM images of silane-functionalized silica: (A) “Silica-Quats” (silica nanoparticles attached with N-Trimethoxysilylpropyl-N,N,N-Trimethylammonium chloride); (B) “Silica-NH_2” (silica nanoparticles attached with (3-Aminopropyl)trimethoxysilane).

1.3.3 Results and Discussion

To examine whether the particles are attached or not, the surface of polyamide membranes were characterized via contact angle measurement (VCA Video Contact Angle System, AST Products, Billerica, MA), X-ray photoelectron spectroscopy (XPS, Surface Science Instrument SSX-100 UHV, monochromated for Al Kα X-rays with 1486.6 eV), scanning electron microscopy (SEM, LEO 1550 FESEM) and Fourier Transform-Infrared Spectroscopy (FTIR, Bruker Optics, Vertex 80v) with an Attenuated Total Reflectance (ATR) prism. Membrane surface roughness was analyzed using a Multimode AFM (Veeco Metrology Group, Santa Barbara, CA) in tapping mode. Also, the durability of the attachment was examined by applying four kind of stresses to the membranes. Chemical stress was applied by contacting the functionalized surfaces for 15 min with a pH 2 solution (HCl), a pH 12 solution (NaOH), or a 0.6 M NaCl solution (approximate the ionic strength of typical seawater), followed by a thorough rinse with deionized water. Physical stress was exerted by immersing the membranes in a sonicating water bath (Fisher Scientific F60) for 7 min. Contact angle measurement, XPS analysis and SEM were again employed to re-evaluate the coated membranes after the stresses.

Contact angles of deionized water on the surface of the silica-coated membranes are shown in Figure 1.8. The contact angle values are average numbers of at least 8 random spots from each sample. Measurements were carried out at room temperature (23 °C). The membranes attached with Silica-Quats (red) and attached with Silica-NH_2 (blue) are much more hydrophilic compared with the untreated polyamide

membranes, from ~ 100 ° to ~ 10 °. Notably, the contact angles of the membranes did not go significantly higher after the four stresses were applied.

The results of the XPS analysis of the surface of the membranes are illustrated in Figure 1.9. In Figure 1.9A the spectra of XPS survey scans are shown for control polyamide membranes (black), membranes coated with Silica-Quats (red) and Silica-NH_2 (blue). Figure 1.9B, C and D illustrate atomic fractions of oxygen (O), carbon (C), nitrogen (N), and silica (Si) relative to the sum of these elements present at the surface for the three different membranes. The elemental fraction was calculated from the survey scans shown in Figure 1.9A. The two coated membranes show the presence of significant amount of silica at their surface (~22%).

Surface morphology and roughness of the membranes were characterized via SEM and AFM analyses, which are shown in Figure 1.10. Surface SEM images of polyamide control membranes are shown in Figure 1.10A and 1.10B with different magnification. Figure 1.10C and Figure 1.10D give the morphology information for the membranes functionalized with Silica-Quats. SEM images for the membranes functionalized with Silica-NH_2 are shown in Figure 1.10E and Figure 1.10F. The AFM tests were conducted by the Elimelech Group at Yale University. AFM images of the polyamide membranes are shown in Figure 1.10G and roughness parameters measured by AFM tapping mode analysis are shown in Figure 1.10H. RMS is root mean square of roughness, $R_{max}/10$ is maximum roughness divided by a factor of 10, R_a is average roughness, and SAD is percentage surface area difference. Black, red, and blue bars refer to neat polyamide membranes, and membranes functionalized with Silica-Quats and Silica-NH_2 particles, respectively. Roughness values are the average

of measurements taken from a total of 12 random spots on 3 separately cast and functionalized sample surfaces. Silica coating made the surface of polyamide smoother.

FTIR spectra for the membranes are presented in Figure 1.11. The appearance of an absorption peak for the coated membranes around 1070-1080 cm^{-1} is commonly attributed to stretching mode of Si-O-Si bonds, indicating the presence of functionalized SiO_2 particles at the membrane surface.

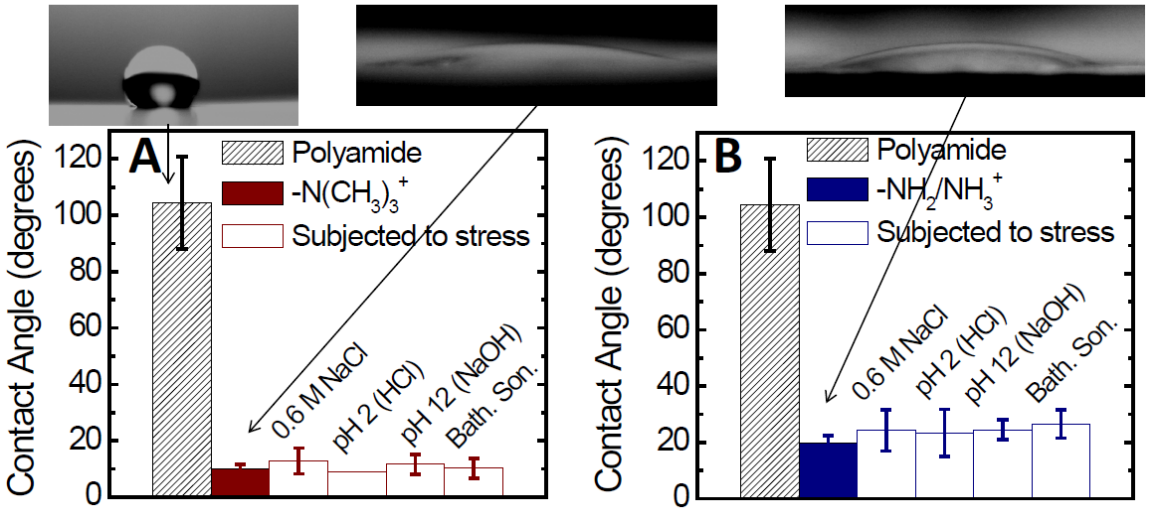

Figure 1.8: Contact angles of deionized water on the surface of (A) Silica-Quats coated polyamide membranes and (B) Silica-NH_2 coated polyamide membranes.

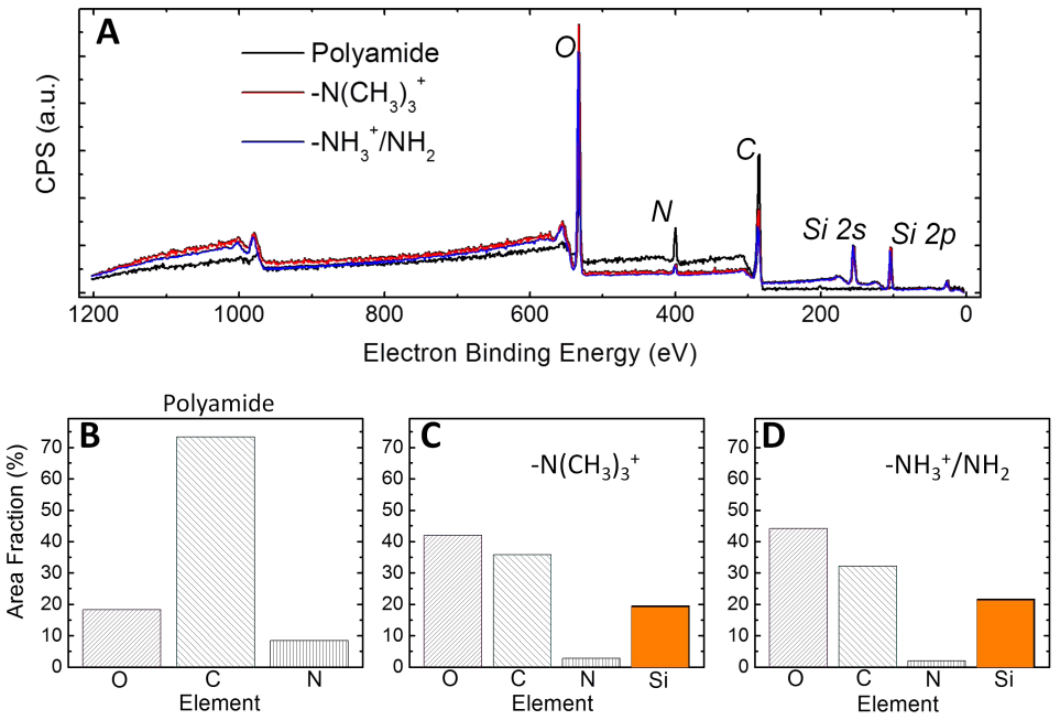

Figure 1.9: XPS analysis of the surface of the membranes. A shows the spectra of survey scans for control (black), Silica-Quats coated (red) and Silica-NH_2 coated membranes (blue). B, C and D correspondingly show the fraction of the elements detected at the surface.

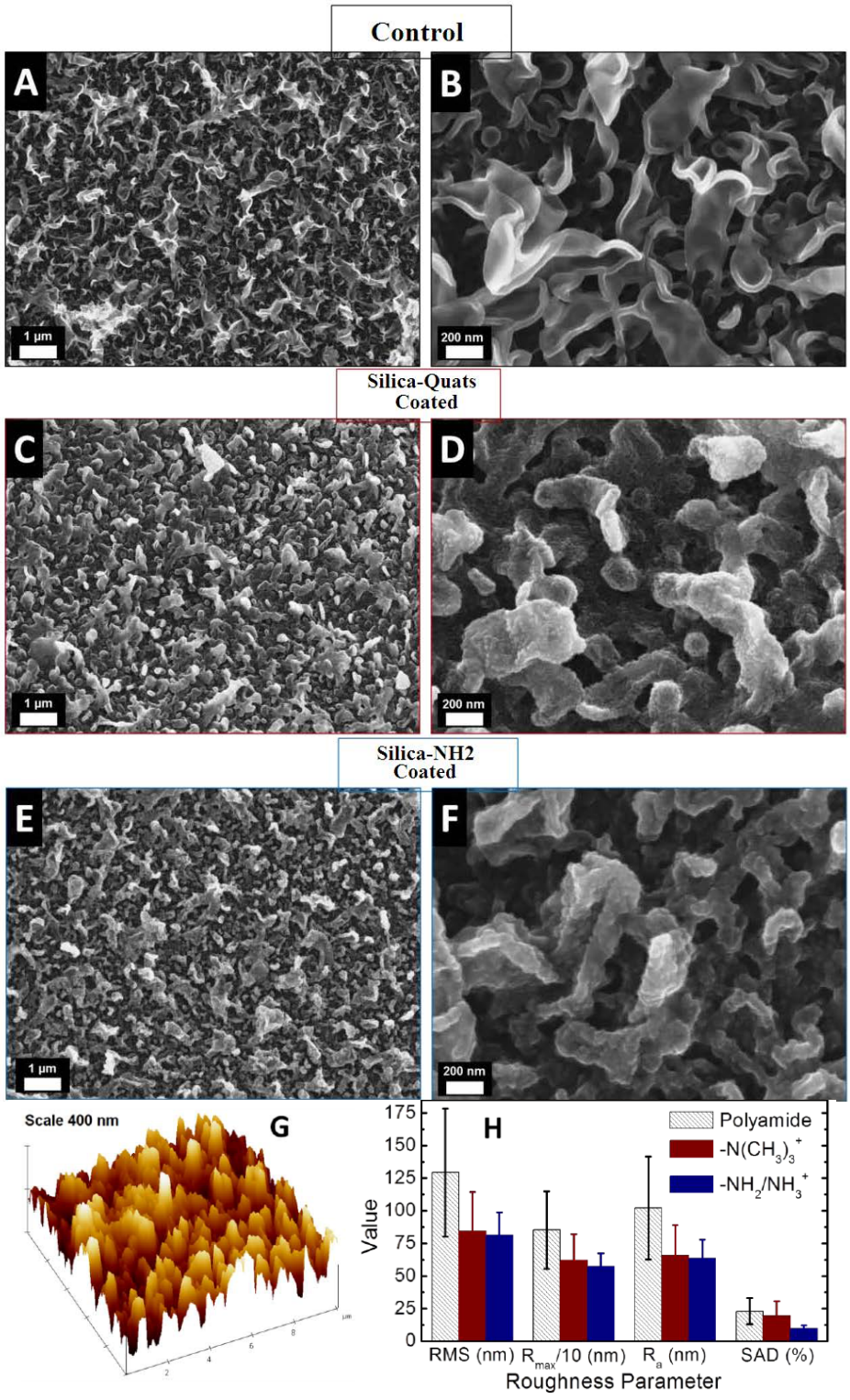

Figure 1.10: SEM and AFM analyses for the surface morphology and roughness of the membranes.

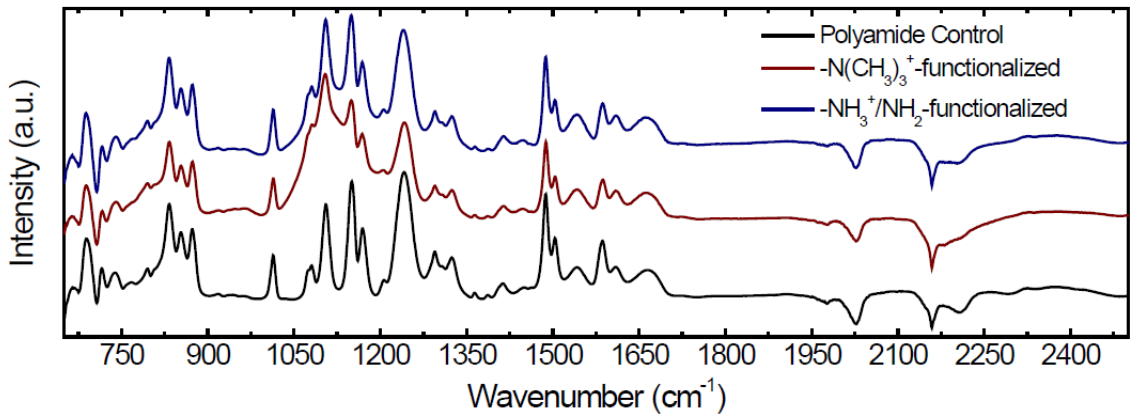

Figure 1.11: FTIR spectra of the silica-coated membranes.

In addition to the contact angle data, the SEM and XPS analysis for the membranes after the physical/chemical stresses do not change much confirming the excellent durability and irreversibility of the modification process. Results of SEM and XPS for the membranes coated with Silica-Quats are presented. The SEM image (Figure 1.12) of Silica-Quats nanoparticles is virtually identical to that before the membranes were subjected to the stresses. The XPS analysis for membranes coated with Silica-Quats after stresses, which is illustrated in Figure 1.13, proves that at the surfaces silica content did not change significantly. The silica fractions on the surface of the membranes remain at the same level.

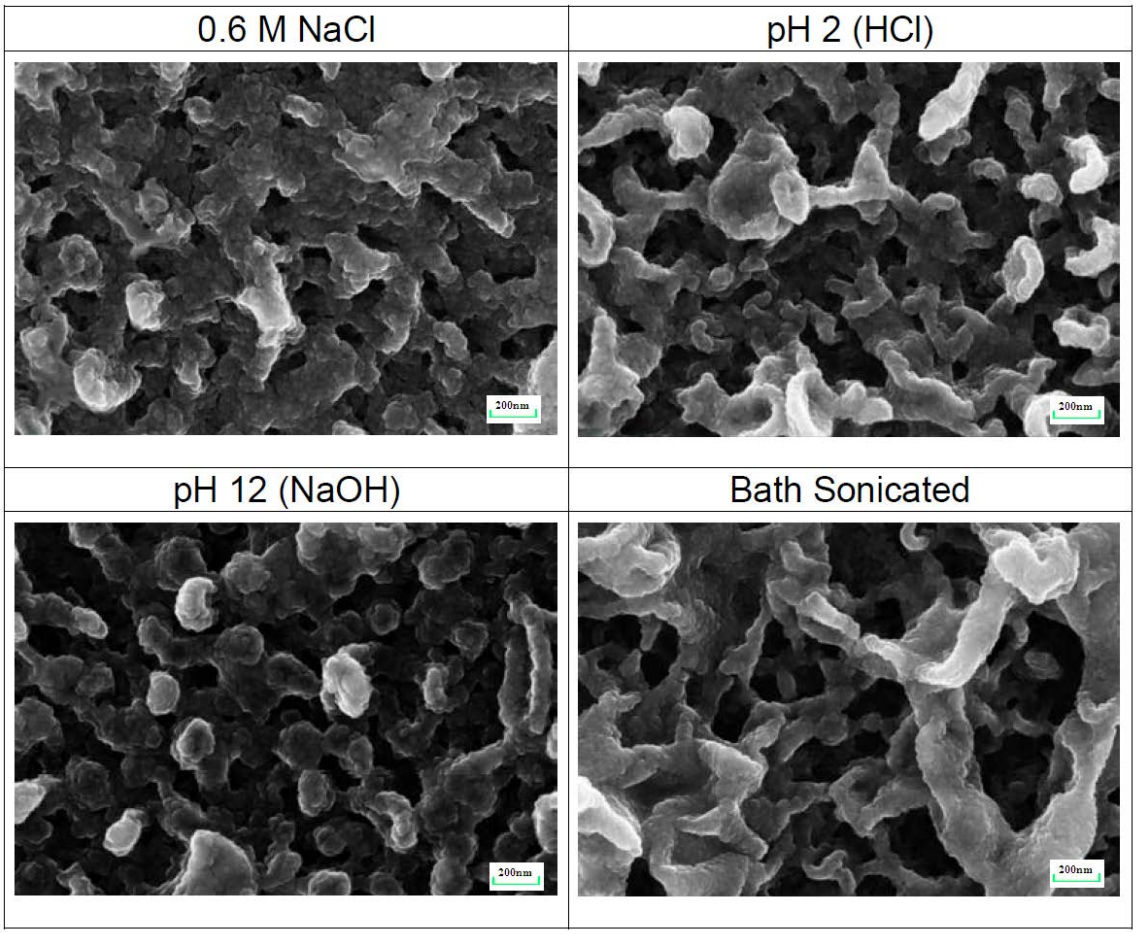

Figure 1.12: SEM images of the membranes coated with Silica-Quats nanoparticles after the application of various stresses.

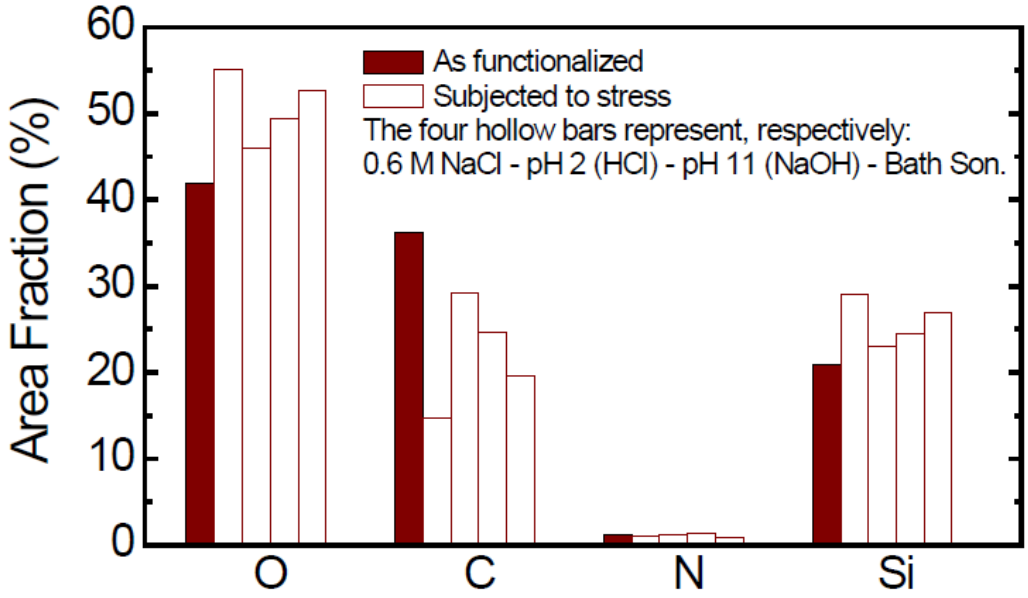

Figure 1.13: XPS analysis of the membranes coated with Silica-Quats nanoparticles after the application of various stresses.

1.3.4 Fouling Behavior

The fouling experiments were done by the Elimelech Group at Yale University. Two kinds of bacteria, namely alginate or bovine serum albumin (BSA) were used in the fouling experiments. The hydrophilic coating of silica can prevent such organic foulants from attaching to the membranes, so AFM was used to measure the adhesive force between the foulants in the bulk solution and the membrane [15]. A particle probe modified from a commercialized SiN AFM probe (Veeco Metrology Group, Santa Barbara, CA) was used for the force measurement. A carboxylate modified latex (CML) particle (Interfacial Dynamics Corp., Portland, OR) with a diameter of 4.0 μm was attached to the tipless SiN cantilever using Norland Optical adhesive (Norland Products, Inc., Cranbury, NJ). Before being immersed in 2000 mg/L model organic foulant solutions of alginate or BSA for 16 hours at 4 °C, the particle probe was cured under UV light for 30 min. The AFM adhesion force measurements were performed in a fluid cell. A simple schematic of the process and results of adhesion force to the two foulants for Silica-Quats coated membranes are shown in Figure 1.14. The curves for control polyamide are represented as black squares. For membranes coated with Silica-Quats red circles are used in the figure. The “No” label stands for measurements where no adhesion force was observed. The test solution for the measurements is synthetic wastewater as described in the experimental section. Measurements were carried out at room temperature (23 °C). When separation distance is around 10 nm, unmodified membranes show strong attraction force to the tip. The silica-coated

membranes show much less attraction force, which proves the modified membranes have reduced affinity to the foulants.

A concern is that water flux may deteriorate by the silica coating. Evaluation of water flux combined with fouling tests for the membranes was subsequently conducted by the Elimelech Group at Yale University. The percentages of water flux in forward osmosis (FO) and reverse osmosis (RO) regarding the silica coating for the membranes are shown in Figure 1.15. The percentage of water flux at the end of the fouling step to the initial water flux is shown as pattern (FO) and hollow (RO) bars. The percentage of water flux recovered after the cleaning step is shown as solid bars. The coated membranes perform better for the two foulants in both FO and RO after fouling. After cleaning, the coated membranes show good recovery ability to almost its initial water flux. The silica coating did not deteriorate the water flux after using but show better fouling behaviors. Temperature was maintained at 25 °C during all the tests.

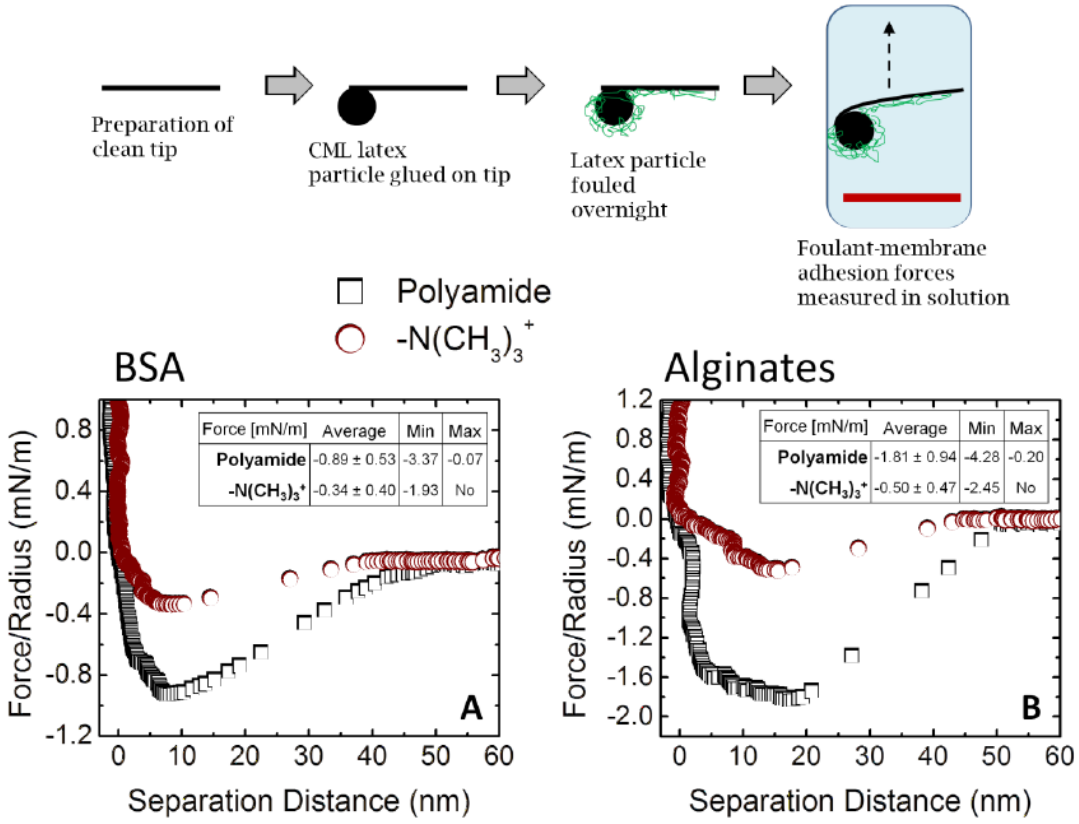

Figure 1.14: AFM retraction curves for foulant-membrane interaction using a A) BSA-fouled tip, and B) alginate-fouled tip.

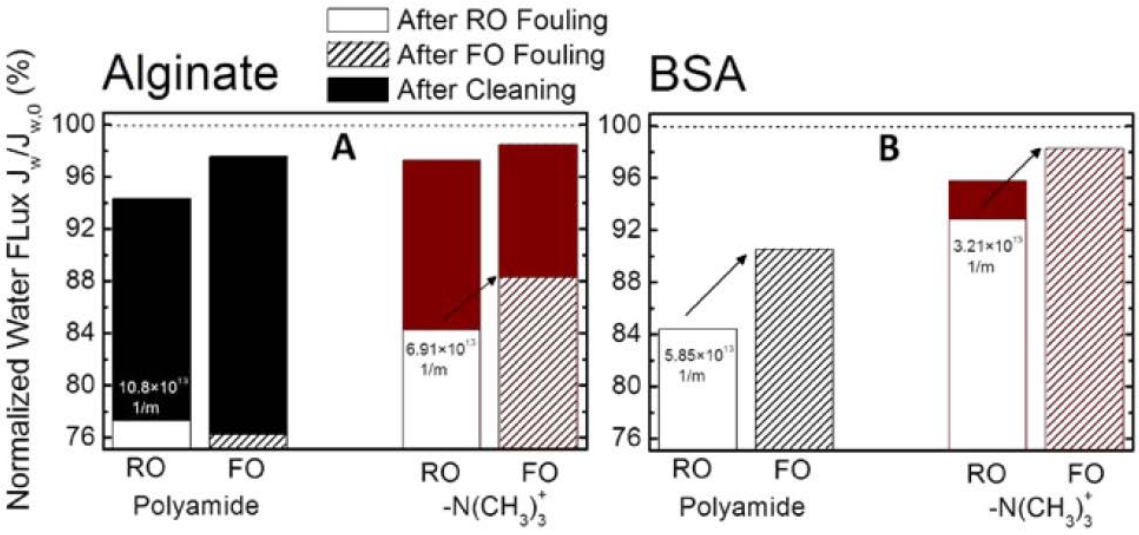

Figure 1.15: The percentage of water flux in FO and RO for the control membranes (black) and the membranes coated with Silica-Quats (red).

1.4 Conclusions

In this chapter, two strategies of modifying the surface of polyamide thin-film membranes by coating with nanoparticles were discussed, with the purpose of promoting the antibacterial property. One is to use poly(ethyleneimine) capped copper nanoparticles taking advantage of the antimicrobial nature of released copper ions in aqueous solution. The other strategy is to render the polyamide surface good hydrophilicity by coating nanoscale silica particles.

Attaching copper particles to the polyamide surface demonstrates feasibility and improvements in reducing fouling. Also, reduced fouling was observed for superhydrophilic membranes coated with silica nanoparticles compared to control polyamide membranes. The coating of silica has been proved durable and irreversible. The fouling resistance and cleaning efficiency of the silica-functionalized membranes was particularly good in forward osmosis.

REFERENCE

[1] Elimelech, M.; Phillip, W. A.; Science **2011**, 333, 712.

[2] Petersen R. J.; Journal of Membrane Science **1993**, 83, 81.

[3] Ridgway, H. F.; Safarik, J.; Biofouling and Biocorrosion in Industrial Water Systems **1991**, 81–111.

[4] Liu, L. F.; Yu, S. C.; Zhou, Y.; Gao, C. J.; Journal of Membrane Science **2006**, 281, 88–94.

[5] Liu, M. H.; Yu, S. C.; Tao, J.; Gao, C. J.; Journal of Membrane Science **2008**, 325, 947–956.

[6] Mauter, M. S.; Wang, Y.; Okemgbo, K. C.; Osuji, C. O.; Giannelis, E. P.; Elimelech, M.; ACS Applied Materials and Interfaces **2011**, 3, 2861– 2868

[7] Zodrow, K.; Brunet, L.; Mahendra, S.; Li, D.; Zhang, A.; Li, Q.; Alvarez, P. J. J.; Water Research **2009**, 43, 715–723.

[8] Basri, H.; Ismail, A. F.; Aziz, M.; Desalination **2010**, 273, 72–80.

[9] Razmjou, A.; Mansouri, J.; Chen, V.; Journal of Membrane Science **2010**, 378 (1-2), 73–84.

[10] Yang, Y.; Zhang, H.; Wang, P.; Zheng, Q.; Li, J.; Journal of Membrane Science, **2007**, 288, 231–238.

[11] Wu, L.; Shamsuzzoha, M.; Ritchie, S. M. C.; Journal of Nanoparticle Research **2005**, 7, 469–476.

[12] Tiraferri, A.; Yip, N. Y.; Phillip, W. A.; Schiffman, J. D.; Elimelech, M.; Journal of Membrane Science, **2011**, 367, 340–352.

[13] Grabarek, Z.; Gergely, J.; Analytical Biochemistry **1990**, 185, 131–135.

[14] Staros, J. V.; Wright, R. W.; Swingle, D. M.; Analytical Biochemistry **1986**, 156, 220–222.

[15] Li, Q. L.; Elimelech, M.; Environmental Science and Technology **2004**, 38, 4683.

CHAPER II

MODIFYING SURFACE OF POLYCARBONATE PLASTIC SHEETS

2.1 Introduction

Polycarbonate belongs to the group of thermoplastic polymers. It is very durable and can be easily molded and thermoformed. Also, polycarbonate can be used in a wide temperature range and has better visible light transmission than normal glass. These excellent characteristics make polycarbonate useful in a wide range of applications, such as improving adhesion of coatings to metals and polymers [1], increasing wettability or printability of polymers [2] , enhancing implantable medical device [3-5], or manufacturing semiconductor devices [6, 7].

However, polycarbonate has low scratch-resistance, which impairs its application in some areas. Further improvements of adhesion and wettability for polycarbonate surface are desired. Current studies have been focused on applying plasma, one of the most versatile methods for surface modification, to the surfaces of polycarbonate [8-11]. Moreover, modification by chemical treatments of polycarbonate has been studied as well [12-14].

In this chapter, ways to coat silica nanoparticles on polycarbonate plastic sheets is proposed, as silica nanoparticles can create a more scratch-resistant and hydrophilic surface without deteriorating the transmission properties of the sheets. Specifically,

the polycarbonate sheets were treated by plasma for introducing polar groups at the surfaces and then were dip-coated in amine-functionalized silica nanoparticles. Various tools were used to examine the coating effectiveness. The polycarbonate sheets are commercial ones provided by SABIC-Innovative Plastics.

2.2 Preparation of Positively Charged Silica Nanoparticles

Three kinds of silane-functionalized silica nanoparticles were tried to coat the polycarbonate sheets. The synthesis processes for two of the silica nanoparticle solutions were described in Chapter I, as called "Silica-Quats" and "Silica-NH_2". The other kind of silica nanoparticles was modified with N-(3-Trimethoxysilylpropyl)diethylenetriamine (Sigma-Aldrich). 3.3 g of this kind of silane was mixed with the diluted commercial silica colloid (~3%, as described in 1.3.1 of previous chapter) as the first step. The mixture was then left on a hotplate stirring at 70ºC for 24 hours before being put in a dialysis tube, yielding the product of silica nanoparticles with three free amino groups at the corona ("Silica-3N") with a pH of ~10. The particles were characterized in the same way as "Silica-Quats" and "Silica-NH_2" through TG/DTA, Zeta potential analysis. Chart 2.1 gives a brief summary of the zeta potentials for each kind of silica nanoparticle solutions under different pH. Thermogravimetric study involved heating (heating rate 5 ºC/min) the freeze-dried particles from room temperature to 700 ºC with continuous flow of air (200 mL/min). Silica-NH_2 lost about 10% of the weight while Silica-Quats and Silica-3N lost about 14%. A simple calculation can be done based on thermogravimetric study: at the

surface of 100 gram silica nanoparticles there are about 0.082 mole, 0.070 mole and 0.069 mole silane molecules attached for Silica-NH_2, Silica-Quats and Silica-3N, respectively.

Table 2.1: Zeta potential (mV) of the silica particles at different pH.

	pH ~ 3.6	pH ~ 5	pH ~ 6	pH ~ 7	pH ~ 8	pH ~ 10
Silica-Quats	50.4±1.06	40.4±1.59			30.5±0.76	
Silica-NH_2		49.5±2.15	29.3±2.45	26.0±1.42		
Silica-3N	42.8±0.99			40.6±0.27		10.9±0.68

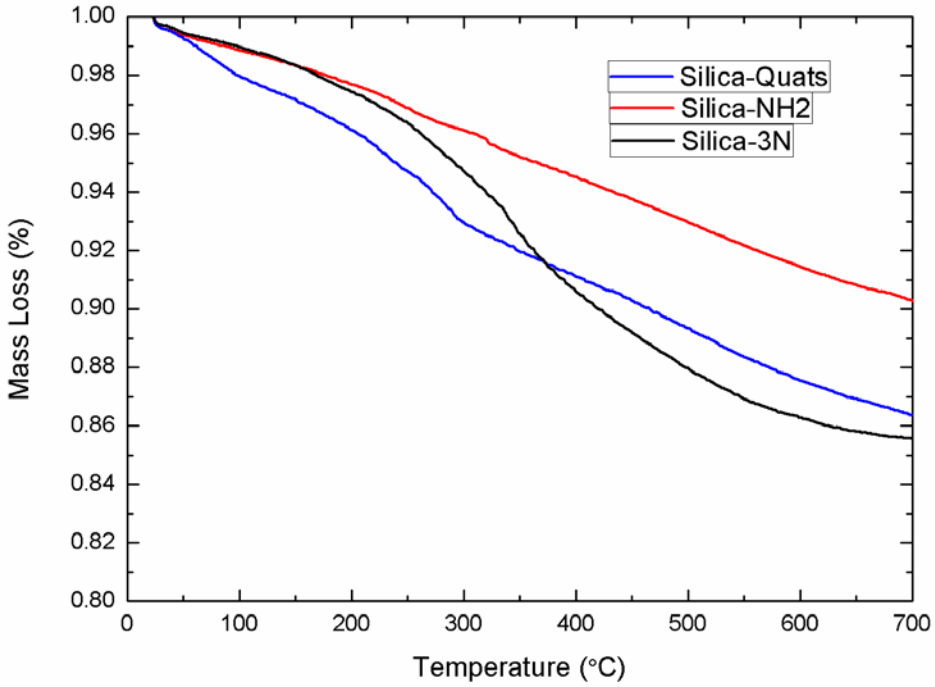

Figure 2.1: Thermogravimetric analysis of Silica-Quats, Silica-NH_2 and Silica-3N.

2.3 Plasma Effect

Unlike the polyamide membranes discussed in the previous chapter, polycarbonate contains much less polar groups that can be utilized for binding. As a result, plasma becomes a good choice for rendering the plastic a more active surface. Nitrogen and Oxygen atmosphere plasma were employed (Plasma apparatus: Glen 1000 Resist Strip). The effect of plasma on the surface of polycarbonate sheets were characterized by contact angle measurement and XPS. A series of plasma treatment time was set to modify the polycarbonate surface, and Figure 2.2 shows the contact angle change of polycarbonate after being exposed to different time periods and power of oxygen plasma treatments. After contacting with the plasma atmosphere in a short time, the polycarbonate sheets showed a sharp drop of water contact angle from ~86º to ~33º, which indicates polar groups were introduced. When the plasma treatment duration became longer, the contact angle did not go down further. As the power was increased above 100 Watts, little change of water contact angle was observed. Most likely, the higher power of plasma merely increased the surface roughness rather than introducing more polar groups. 100 Watts of plasma was mainly used in further experiments. Combined with wide survey scan for determining oxygen content at the plasma-treated polycarbonate surface, high-resolution XPS analysis was used for analyzing C 1s peak. The high-resolution result was analyzed using the software CasaXPS. Peak fitting and cumulative areas of the fitted peaks were taken into account for calculating the percentage of each chemical group (one example of polycarbonate treated by oxygen plasma at 100 Watts for 60s is shown in Figure 2.3).

The XPS data is presented in Table 2.2. From the XPS analysis, oxygen atomic fraction at the surface increase from ~16.4% to ~25%. Longer plasma duration did not significantly increase the amount of double-bond groups (C=O, O-C=O). 15 seconds of plasma time was consequently selected for follow-up experiments, because the contact angle would increase very quickly in a short time after plasma treatment.

Table 2.2: High-resolution XPS data for C 1s of oxygen plasma-treated polycarbonate sheets, in unit of percentage (%)

		Virgin PC	O_2, 100W,15s	O_2, 100W,30s	O_2, 100W,60s	O_2, 100W,120s	O_2, 100W,300s
Survey Scan, O%		16.4	24.6	25.0	26.0	24.6	24.8
Hi-Res Scan for C 1s	C-C sp^2 (~284.5eV)	52.8	69.6	68.8	66.9	72.6	71.9
	C-C sp^3 (~285.0eV)	26.1					
	C-O (~286.1eV)	13.0	9.4	10.9	11.6	7.1	8.7
	C=O (~287.2eV)	/	6.7	6.6	7.4	7.0	6.1
	O-C=O (~288.5eV)	/	7.8	6.7	8.1	7.4	7.7
	Carbonate (~290.5eV)	8.1	6.5	7.0	6.0	5.9	5.6

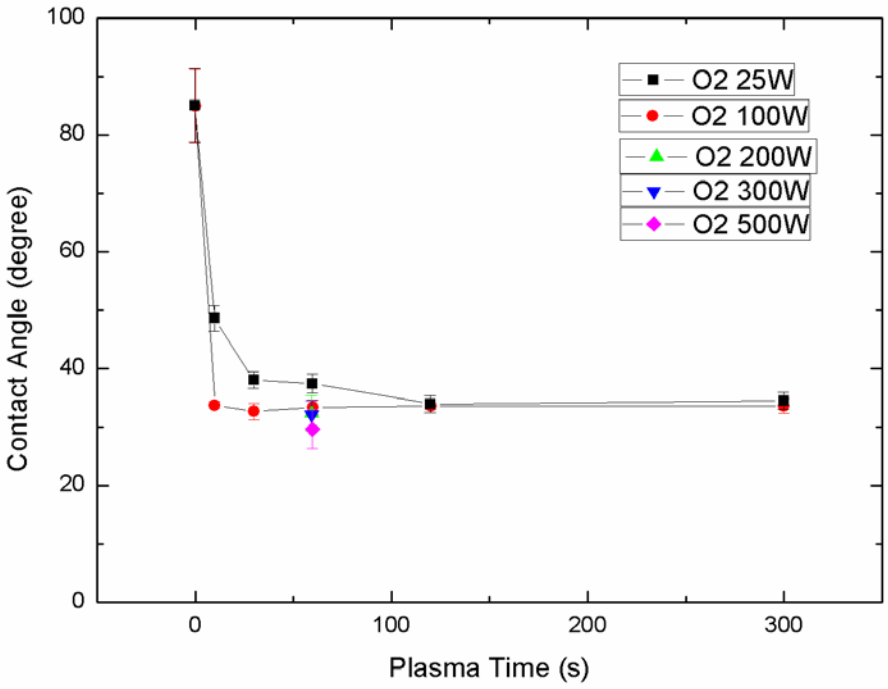

Figure 2.2: Contact angle of polycarbonate surface under different treatment durations of oxygen plasma.

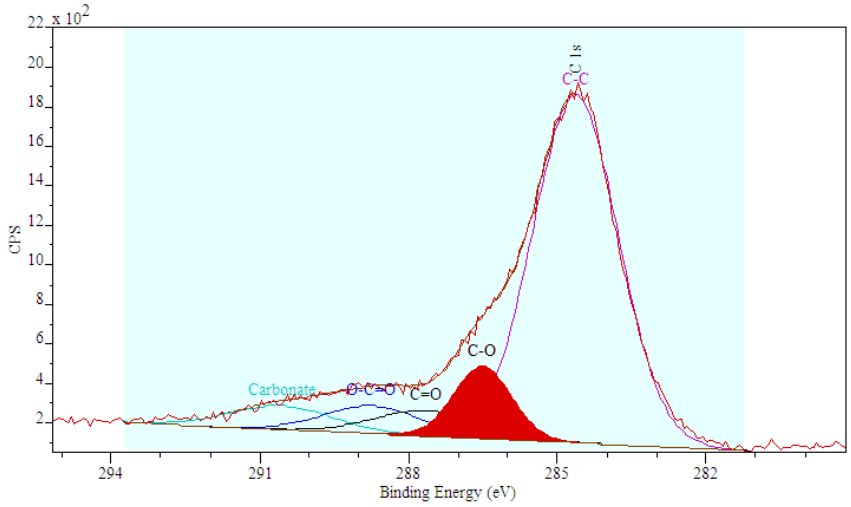

Figure 2.3: High-resolution XPS analysis for C 1s of oxygen plasma treated polycarbonate at 100 Watts for 60s.

2.4 Results and Discussion

Solution-based dip-coating was still the primary method for coating the polycarbonate sheets. Plasma-treated polycarbonate sheets were directly immersed in the silica solutions (without changing pH). Contact angle measurement, XPS, and SEM were again used to characterize the coated surfaces of polycarbonate sheets.

Contact angle measurement was conducted for the samples that were freshly prepared, rinsed once in a few days and aged in laboratory condition for about 30 days, and sonicated in deionized water for 5min after the 30-days aging (Figure 2.4). The virgin polycarbonate sheet has a water contact angle of ~86º. For the samples coated with Silica-Quats and Silica-NH_2, contact angle increased after the samples were treated by aging and sonicating. When coated with Silica-3N, the samples performed better after the treatments, keeping water contact angle below 60º.

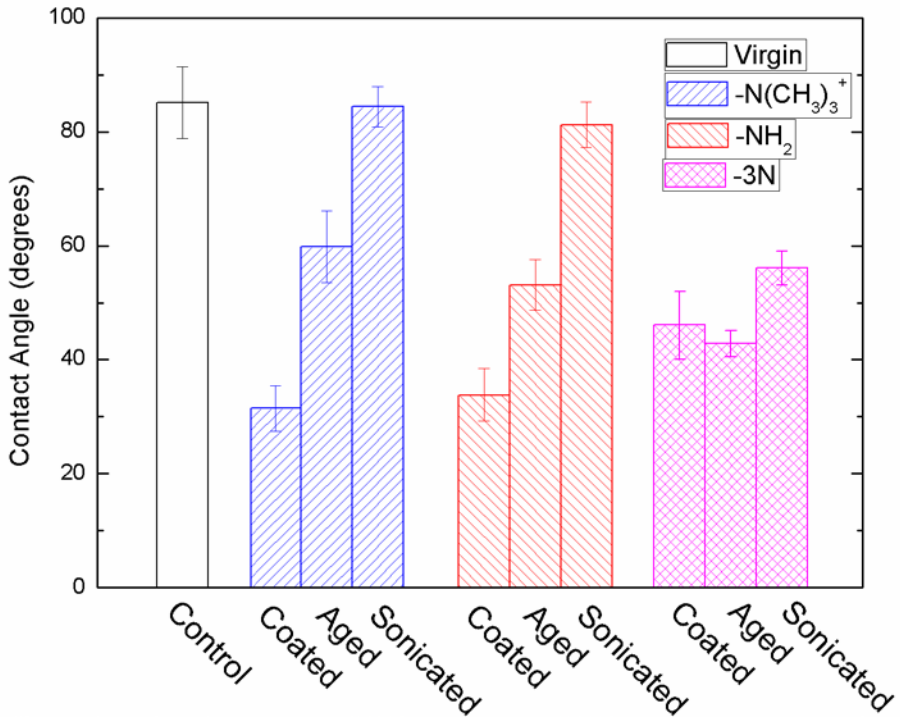

Figure 2.4: Contact angle for virgin polycarbonate (white) and polycarbonate coated with "Silica-Quats" (blue), "Silica-NH_2" (red) and "Silica-3N" (magenta).

Survey scan of XPS analysis was further used to confirm the existence of silica layers at the polycarbonate surface, which is shown in Chart 2.3. Virgin polycarbonate showed no signal of Si. When right after coated with silica nanoparticles, all the samples showed a Si fraction above 20% and which decreased after aging for about 30 days in normal laboratory conditions. Sonication made a large portion of the particles finally detached from the polycarbonate sheets, with a Si fraction of around 10% at the surfaces.

Table 2.3: XPS analysis of Si content for polycarbonate sheets, in unit of percentage (%).

	Right after coated	Aged for ~30 days	Sonicated in water
Silica-Quats coated	24-28	15-18	6-9
Silica-NH_2 coated	24-28	15-18	6-8
Silica-3N coated	22-26	16-19	12-14

SEM images of the coated polycarbonate sheets were shown in Figure 2.5. When the samples were initially coated, more than one layer of silica nanoparticles were observed no matter what kind of silane was used for particle functionalization (Figure 2.5A showed the freshly prepared Silica-NH_2 coated sample). After aging, only one layer of silica remained for Silica-Quats coated and Silica-NH_2 coated samples (Figure 2.5B showed the Silica-NH_2 coated sample after aging). For Silica-3N coated samples, still some island-like extra silica was attached the bottom one layer (Figure 2.5C).

These excess possibly resulted from the low zeta potential of Silica-3N partciles (about 10.9 mV at pH 10), which makes the particles stick together more firmly. This may explain why after aging Silica-3N coated samples presented a relatively low water contact angle.

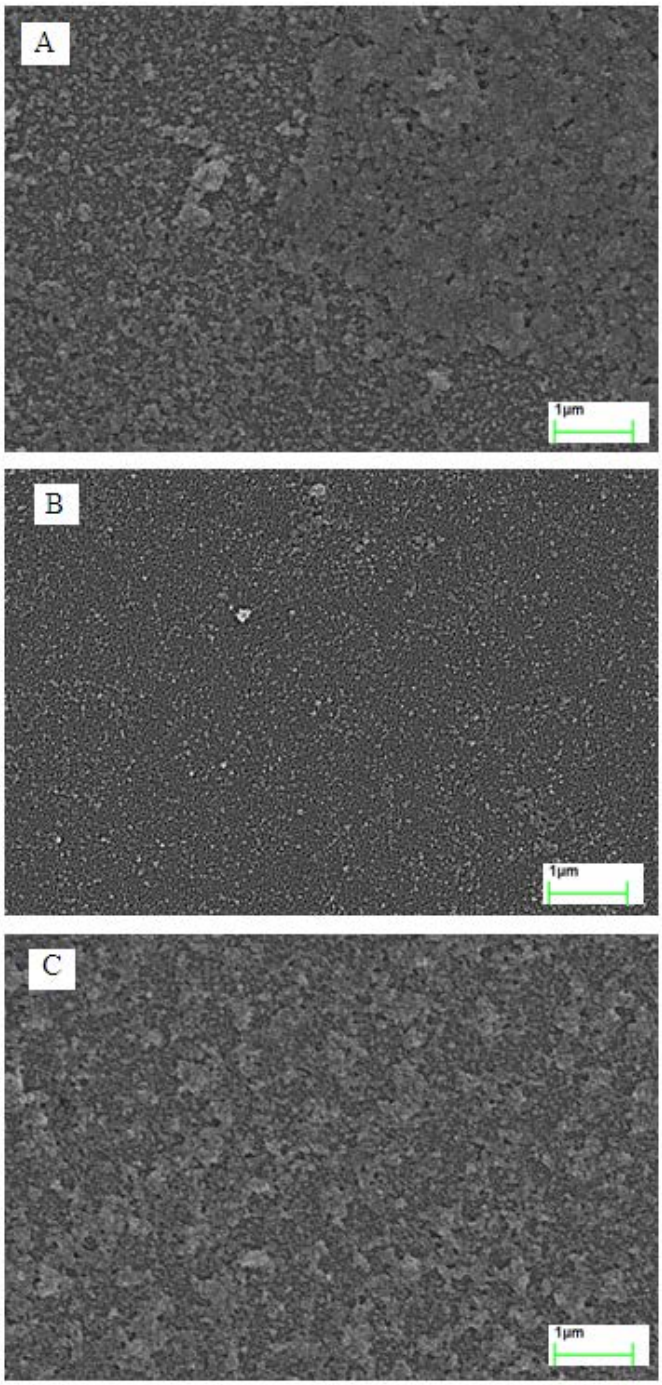

Figure 2.5: SEM images of (A) polycarbonate freshly coated with Silica-NH_2, (B) Silica-NH_2 coated polycarbonate after aging and rinsing, (C) Silica-3N coated polycarbonate after aging and rinsing.

After sonication, silica nanoparticles detached from the surface, as indicated by higher contact angle and lower elemental fraction of Si. Nevertheless, Silica-3N coated samples performed better than the other two groups (Silica-Quats coated and Silica-NH_2 coated) even after sonication treatment. Two reasons may lead to this behavior: 1. the excess silica of Silica-3N protects the linkage between the bottom layer and the polycarbonate surface during sonication; 2. Silica-3N silica was synthesized by a longer chain of silane with more amino groups, which contributes to a stronger binding (as binding possibility increased) between the bottom layer and the polycarbonate surface.

A layer-by-layer method was designed to artificially increase the thickness of coating and then examine the cause. Carboxylic group terminated silane (Carboxyethylsilanetriol, Sodium Salt, 25%, Gelest) was used to functionalize the silica nanoparticles (Silica-COOH), akin to the amino groups functionalized silica. The particle has a negative zeta potential of about -24.4mV at pH 8. A schematic of the layer-by-layer coating method is shown in Figure 2.6. The samples were coated with Silica-NH_2 as the first layer after plasma treatment, and Silica-COOH was deposited afterwards. The differently charged particles were alternately used for depositing more layers. The samples were rinsed by deionized water before depositing next layer.

Figure 2.7 shows the SEM appearance of the sample deposited by Silica-NH_2 and Silica-COOH for “4 layers” (Two layers of Silica-NH_2 and two layers of Silica-COOH were built alternately) before aging. Rougher surface than the sample shown in Figure 2.5B can be seen, indicating more than one layer of silica particles. The contact angle

data for samples deposited by Silica-NH_2 and Silica-COOH is presented in Figure 2.8. More deposited layers showed very limited help in preserving a relatively low water contact angle. The binding strength between the bottom layer and the surface plays a critical role.

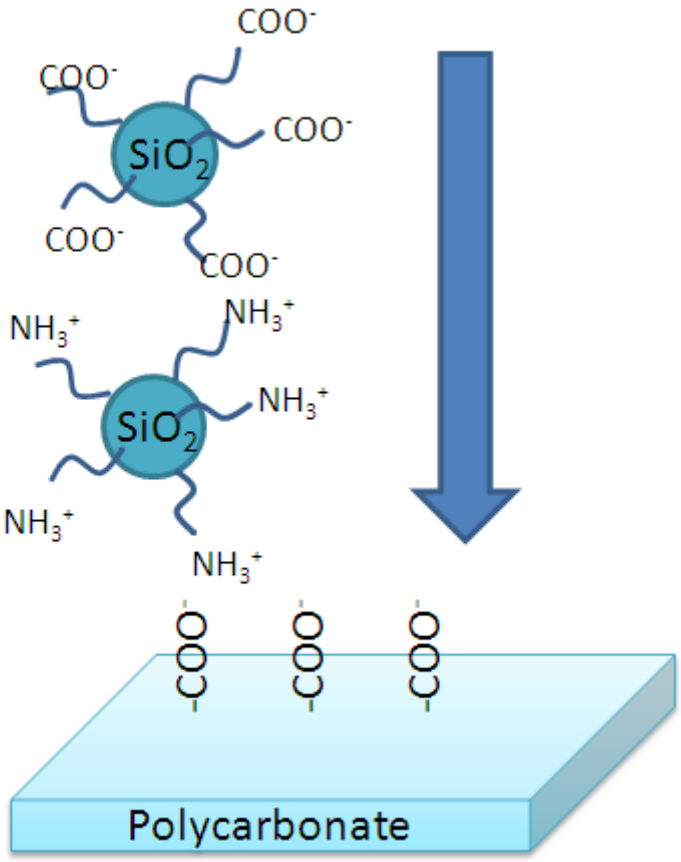

Figure 2.6: Schematic of "layer-by-layer" method to artificially add layers of silica on polycarbonate sheets.

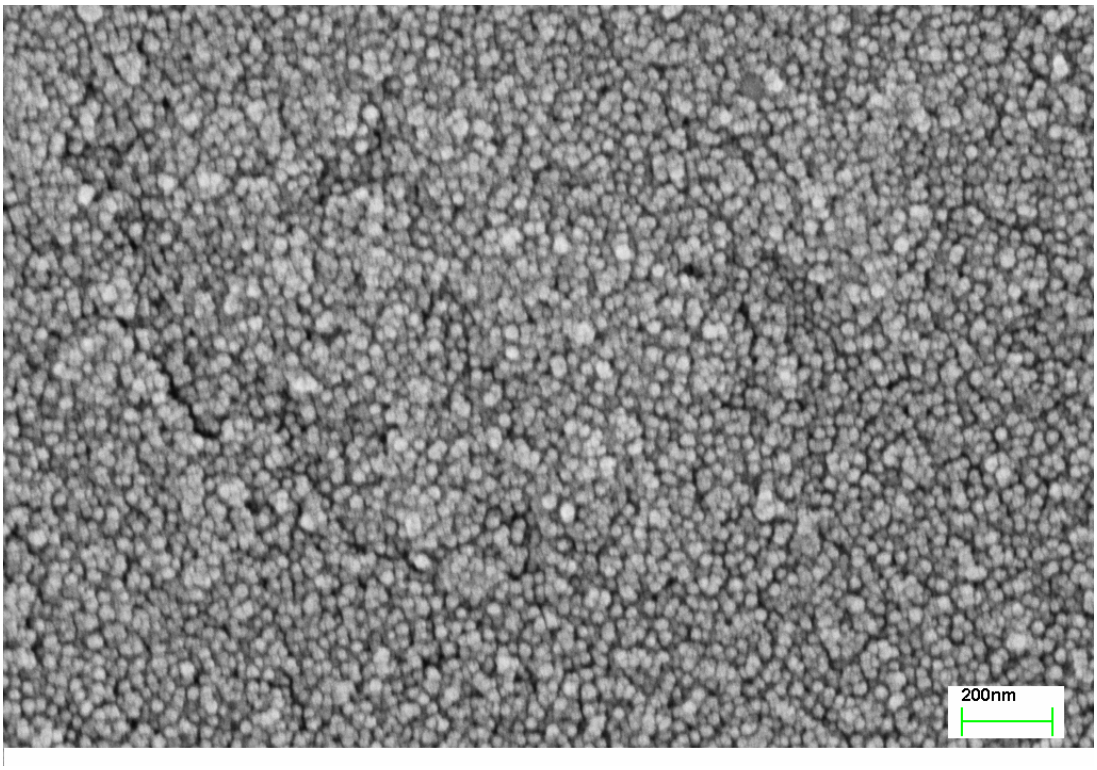

Figure 2.7: SEM image of the “4 layers” coating of silica on polycarbonate sheets.

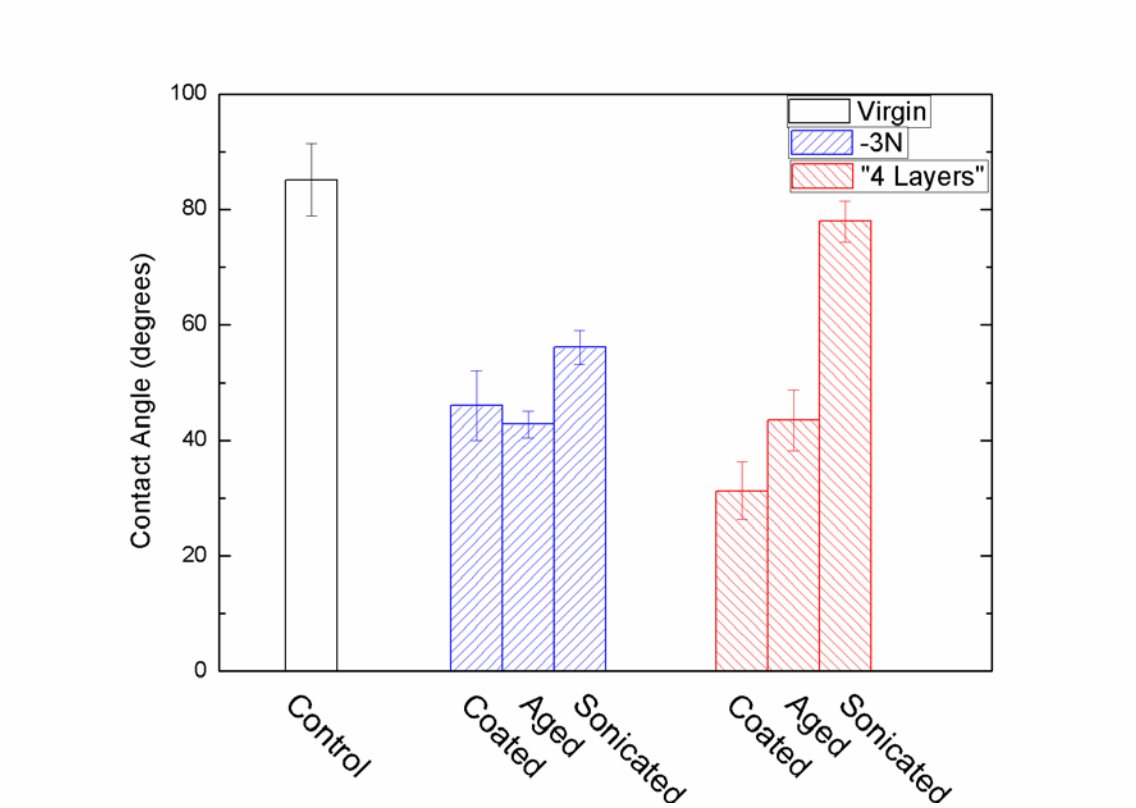

Figure 2.8: Contact Angle of polycarbonate samples coated by the “layer-by-layer” method with different layers.

Similar study was conducted for nitrogen plasma atmosphere. The samples treated by nitrogen plasma showed nitrogen-contained groups (-CN, -CNO, etc.), and also showed some improvements but not significant. Unlike the polyamide membranes discussed in the previous chapter, the polycarbonate does not initially have free carboxylic groups. The plasma-induced carboxylic groups could be in a low density. Also, unlike polypropylene [15, 16], polycarbonate are not so active when exposed in plasma due to the molecule structure of polycarbonate. Further study is needed for a more durable and resistant coating.

2.5 Conclusions

In this chapter, plasma treatment and coating of silica nanoparticles on polycarbonate plastic sheets are investigated. Plasma can induce oxygen-contained polar groups at the polycarbonate surfaces, as proved by high-resolution XPS analysis. The oxygen-contained groups were then used for tethering amine-terminated silica nanoparticles via dip-coating method.

Silica-Quats and Silica-NH_2 particles showed limited durability on the surfaces while Silica-3N performed better. A layer-by-layer method was tried. From the results, more than one layer is not the primary reason for better durability. Stronger binding between the bottom layer and the plastic surface is critical.

REFERENCES

[1] Liston, E.; Martinu, L.M.; Wertheimer, M.R.; Journal of Adhesion Science and Technology **1993**, 7, 1091–1127.

[2] Wu, S.; Polymer Interface and Adhesion, Marcel Dekker, New York, **1982**, pp. 279–336.

[3] Pedrosa, P; Chappe, J. M.; Fonseca, C; Machado, A. V.; Nobrega, J. M.; Vaz, F.; Plasma Processes and Polymers **2010**, 7 (8): 676-686.

[4] Chu, P. K.; Chen, J. Y.; Wang, L. P.; Huang, N.; Materials Science and Engineering **2002**: Rep. 36 (5&6) 143–206.

[5] Schroder, K.; Meyer, A. P.; Keller, D.; Besch, W.; Babucke, G.; Contributions to Plasma Physics **2001**, 41, 562.

[6] Lin, Y. S.; Weng, M. S.; Chung, T. W.; Huang, C.; Surface and Coatings Technology **2011**, (13-14), 3856-3864.

[7] Schmid, H.; Kegel, B.; Petasch, W.; Liebel, G.; Proceedings of Joint 24th International Conference Microelectronics (MIEL) and 32nd Symposium Devices Materials SD'96, Nova Gorcia, Slovenia, **1996**, pp. 17–35.

[8] Sharma, R.; Holcomb, E.; Trigwell, S.; Mazumder, M.; Journal of Electrostatics **2007**, 65, 269.

[9] Kitova, S.; Minchev, M.; Danev, G.; Journal of Optoelectronics and Advanced Materials **2005**, vol. 7, no. 5, pp. 2607–2612.

[10] Hofrichter, A.; Bulkin, P.; Drevillon, B.; Journal of Vacuum Science Technology **2002**, Volume 20, Issue 1, pp. 245-250.

[11] Keil, M.; Rastomjee, C. S.; Rajagopal, A.; Sotobayashi, H; Bradshaw, A. M.; Lamont, C. L. A.; Gador, D.; Buchberger, C; Fink, R.; Umbach, E.; Applied Surface Science **1998**, 125:273–286.

[12] Li, C.; Wilkes, G. L.; Journal of Inorganic and Organometallic Polymers **1998**, Vol. 8, No. 1.

[13] Cardwell, J. R.; Jackson JR, W. J.; Journal of Polymer Science Part C: Polymer Symposia **1968,** Volume 24, Issue 1, NO. 24, PP. 15-23.

[14] Wu, Linda Y. L.; Boon, L,; Chen, Z.; Zeng, X. T.; Thin Solid Films **2009**, 517, 4850–4856

[15] Grace J. M.; Gerenser, L. J.; Journal of dispersion science and technology **2003**, Vol. 24, Nos. 3 & 4, pp. 305–341.

[16] Fang, J.; Kelaraskis, A.; Estevez, L.; Wang, Y.; Rodrigues, R.; Giannelis, E. P.; Journal of Materials Chemistry **2010**, 20, 1651-1653.